https://doi.org/10.1016/j.jorganchem.2017.06.006

One-pot synthesis of ferromagnetic FePd nanoparticles from single-source organometallic precursors and size effect of metal fraction in polymer chain

Zhengong Meng [a, b] , Guijun Li [c] , Nianyong Zhu [a, b] , Cheuk-Lam Ho [a, b, *] , Chi-Wah Leung [c], [**], Wai-Yeung Wong [a, b, d, ***]

a Institute of Molecular Functional Materials, Department of Chemistry, Hong Kong Baptist University, Waterloo Road, Kowloon Tong, Hong Kong, China

b HKBU Institute of Research and Continuing Education, Shenzhen Virtual University Park, Shenzhen, 518057, China

c Department of Applied Physics, The Hong Kong Polytechnic University, Hung Hom, Hong Kong, China

d Department of Applied Biology and Chemical Technology, The Hong Kong Polytechnic University, Hung Hom, Hong Kong, China

E-mail addresses:

clamho@hkbu.edu.hk (C.-L. Ho),

dennis.leung@polyu.edu.hk (C.-W. Leung),

rwywong@hkbu.edu.hk, wai-yeung.wong@polyu.edu.hk (W.-Y. Wong)

Highlights

• Bimetallic complexes containing Fe and Pd were prepared.

• Ferromagnetic FePd nanoparticles were synthesized by one-pot pyrolysis of these single-source precursors.

• The size of FePd nanoparticles was tuned by controlling the ratio of the metal fraction in the precursors.

Keywords
Bimetallic compound, Ferromagnetic, Nanoparticle, Metallopolymer, Synthesis

Abstract

The accurate regulation of the size of the ferromagnetic nanoparticle synthesized from the one-pot pyrolysis of metallopolymer is a challenging topic to date. A bimetallic complex **TPy-FePd-1** was prepared and used as a single-source precursor to synthesize ferromagnetic FePd nanoparticles (NPs) by one-pot pyrolysis. The resultant FePd NPs have a mean particle size of 19.8 nm and show a coercivity of 1.02 kOe. In addition, the labile ligand NCMe in **TPy-FePd-1** was easily substituted by a pyridyl group. A random copolymer **PS-P4VP** was used to coordinate with **TPy-FePd-1**, and the as-synthesized metallopolymer made the metal fraction disperse evenly along the flexible chain. Investigation of FePd NPs from the bimetallic polymers with different metal fractions was also made, and the size of the resultant nanoparticles could be easily controlled by tuning the metal fraction in the polymer.

1. Introduction

Nanomaterials, characterized by a size of 100 nm or smaller in at least one dimension, are of intense current interest for a variety of applications due to their unusual physical and chemical properties such as mechanical [1], [2], [3], catalytic [4], optical [5], [6] and magnetic properties [7], [8], [9], etc. In comparison with the bulk counterparts, the specific performance of nanomaterials could be ascribed to the so-called "quantum size effects" at the nanoscale [10]. Hence, it is crucial to study nanomaterials with controllable size.

The demand for magnetic recording media of higher density is one of the fundamental motivations for the recent interest in hard magnetic NPs that are characterized by high magnetocrystalline anisotropy energy. As one of the candidates for a high density magnetic storage media, FePd NPs with high magnetocrystallic anisotropy and chemical stability have attracted much attention [11]. The hard FePd NPs show a high K_u of 9×10^5 erg/cm^3, and the coercivity of the resultant particles is revealed to be closely related to their size. The decrease in sample size induces a change from the multivariant mode to the single variant mode in which the strain energy is large [12].

Considerable efforts have been made in recent years in developing methods for the synthesis of single domain magnetic FePd NPs with well-defined size and shape [13], [14], [15], [16], [17]. In general, the physical deposition method was proved to be effective to control the atomic ratio and tune the particle size, which also afforded a good way in preparing FePd NPs [18], but it is not easy to disperse the resultant NPs in various liquid media. By contrast, solution phase chemical synthesis was successfully used to prepare monodisperse metallic NPs [19], and Sun et al. further developed the synthesis of FePt NPs [20]. The method was widely recognized and also extended to synthesize other NPs such as FePd [21], FeCo [22], CoPt [23] NPs, etc. In

particular, thermal decomposition of $Fe(CO)_5$ or $Fe(acac)_3$ coupled with reduction of $Pd(acac)_2$ was still widely used to prepare FePd NPs [24], [25]. The chemical reduction routes were successfully to synthesize monodisperse alloy NPs, but post-annealing at high temperature was needed to obtain the fct phase, and the two separate Fe-source and Pd-source were not good for controlling the atomic ratio due to their different decomposition temperatures.

Organometallic complexes were widely used in various areas, such as optical, electrical or magnetic applications, etc [26], [27], [28], [29], [30]. Single-source organometallic precursors were proposed to fabricate magnetic FePd NPs, which had been proved successfully in synthesizing FePt NPs [31], [32], [33]. Manners et al. reported the Fe,Pd-containing chelated complexes which nicely synthesized the mixed-metal FePd alloy NPs in moderate yields (ca. 55–60%) at relatively low temperatures [34].

In our previous work, Fe,Pt-containing metallopolymers were identified to be a novel type of single-source precursors, and the ferromagnetic $L1_0$-FePt NPs could be obtained by a one-step pyrolysis [35], [36], [37], [38]. In addition, the size of the resultant NPs was also easily controlled by tuning the pyrolysis condition [39], [40]. Herein, we extend the method for preparing another type of ferromagnetic alloy NPs, namely FePd NPs. Fe,Pd-containing organometallic compounds with equal atomic ratio of Fe to Pd will be prepared and used as single-source precursors to synthesize FePd NPs by a one-pot method. The size of FePd NPs can also be easily controlled by tuning the steric structure of the precursors and the metal fraction in the polymers. Furthermore, the size effect on the magnetic properties of the NPs has been investigated in the present study.

2. Results and discussion

2.1. Synthesis and characterization of Fe,Pd-containing single-source precursors

In the present study, the ferrocene-substituted terpyridine ligand 4′-(ferrocenyl)-[2,2′:6′,2″]terpyridine was synthesized by a one-step reaction in good yield (Scheme 1). The ligand reacted with $Pd(OAc)_2$ in dry MeCN first and the mixture was subsequently treated with $HBF_4{\cdot}Et_2O$ to obtain [4′-ferrocenyl-(NˆNˆN)$Pd(NCCH_3)$]$(BF_4)_2$ **TPy-FePd-1** in quantitative yield. The acetonitrile ligand in **TPy-FePd-1** was displaced by DMSO upon dissolution, which was identified by the appearance of free CH_3CN observed in the ^1H NMR spectrum.

Single crystals suitable for X-ray diffraction (XRD) analysis was obtained by slow evaporation of Et_2O into the acetonitrile solution of **TPy-FePd-1**. Fig. 1 depicts the structure of the cation of **TPy-FePd-1**. Selected bond lengths and angles are given in Table 1. The molecular structure shows a distorted square-planar geometry of the palladium(II) center and a pendant ferrocenyl unit. The acetonitrile ligand is connected to the metal by a dative bond in the solid state and the bond length of Pd-N(4) is 2.015(3) Å.

To further establish the ease of displacement of the MeCN ligand from the coordination sphere, adduct **TPy-FePd-1** was treated with an equivalent of 4-*tert*-butylpyridine to produce the model complex **TPy-FePd-2**. As expected, this reaction produced a compound with a *tert*-butyl group, and the assignment was confirmed by ^1H NMR spectroscopy, which showed a strong -$C(CH_3)_3$ signal at δ = 1.42 ppm.

The random block copolymer **PS-P4VP** was synthesized by the free radical polymerization, and further treated with **TPy-FePd-1**, in which the pyridyl group could be easily coordinated to the Pd complex to obtain a new metallopolymer. The metal fraction in polymer was able to be tuned,

and hence, **P1**, **P2** and **P3** with 5 wt%, 10 wt% and 20 wt% of metal fractions, respectively were prepared and characterized by ^{1}H NMR spectroscopy.

2.2. Preparation of FePd NPs from TPy-FePd-1

The organometallic complex **TPy-FePd-1** was selected as the single-source precursor to prepare FePd NPs by the one-pot pyrolysis at high temperature under a getter gas atmosphere (95:5 Ar/H_2). The precursor was first pyrolyzed for 1 h at 500 °C, and then annealed at higher temperature (800 °C) to enhance the ordering of FePd NPs. The resultant FePd NPs were assigned as **FePd-1**.

The morphology and lattice fringes of the resultant **FePd-1** NPs were characterized by transmission electron microscopy (TEM). As depicted in Fig. 2a and b, the NPs were evenly embedded in the carbon matrix with a uniform spherical shape. The mean size was about 19.8 nm with a narrow size distribution (Fig. 2c), which was statistically analyzed from the TEM images. In addition, the obvious lattice fringe of 0.227 nm, corresponding to the (111) plane, suggests that the resultant NPs had high crystallinity. The atomic ratio of Fe to Pd was about 49:51, as determined by energy dispersive X-ray (EDX) analysis (Fig. 2d), which was very close to the theoretical composition.

The powder XRD pattern of **FePd-1** NPs confirmed that the as-synthesized NPs had a chemically ordered face-centered tetragonal (fct) structure (Fig. 3) according to the characteristic peaks (001) and (110) of the fct phase. Also, the splitting of the peaks (200) and (220) appeared, which further identified the phase of the NPs. Furthermore, the size of **FePd-1** NPs calculated from the (001) peak according to the Scherrer's equation is consistent with the TEM analysis.

The magnetic hysteresis loop was measured at room temperature by vibrating sample magnetometer (VSM) (Fig. 4). The loop implied the ferromagnetic properties of **FePd-1** NPs.

When 2 T of an external magnetic field was applied, the particles reached saturation with a magnetic moment of 13.3 emu/g. However, the remnant moment of 4.2 emu/g remained unchanged after removing the applied field, and another magnetic field in the opposite direction should be introduced to cancel the remnant magnetic moment. Thus, the coecivity was about 1.02 kOe. The ferromagnetic behavior further matched with the fct structure as deduced from the TEM images and XRD analysis.

2.3. Size-tunable FePd NPs synthesized from P1–P3

Well-defined FePt NPs can be easily synthesized from the polymeric precursors, and the size of the NPs was found to be tunable by controlling the pyrolysis conditions or the ratio of the metal source to polymer [41]. However, it is still rare to prepare other types of NPs using the similar precursor approach. In particular, FePd NPs, as the counterpart of FePt NPs, have the similar microstructure and magnetic properties. In this study, in order to investigate the effect of the polymeric backbone on forming FePd NPs and controlling the size of the as-synthesized NPs, the polymers **P1**, **P2** and **P3** were also pyrolyzed to prepare FePd NPs named as **FePd-2**, **FePd-3** and **FePd-4**, respectively.

The resultant NPs were characterized by TEM (Fig. 5). The low-resolution images demonstrated the morphology of the as-synthesized FePd NPs. The particles were evenly embedded in the carboneous matrix to maintain the stability, which was consistent with **FePd-1** NPs. The size of the particles was statistically analyzed from the TEM images, as shown in Fig. 5b,d,f. The mean size corresponding to **FePd-2**, **FePd-3** and **FePd-4** NPs was 10.5 nm, 14.4 nm and 17.5 nm, respectively. These average sizes are smaller than that of the **FePd-1** NPs, and the particle was grown with larger size as the metal fraction in polymer increased. The difference in size can be assigned to the different steric structure of the organometallic polymer precursors. As shown in

the crystal structure, **TPy-FePd-2** in the solid state has a square-planar structure, which easily gives rise to the molecular interactions by π-π stacking. The stacked behavior in the precursors made the metal source closely integrated, so that Fe and Pd atoms can better form alloys during nucleation. However, since the metal fraction in polymer was randomly dispersed along the polymer chain, the planar structure of the metal fraction was more separated and the stacking behavior became less significant.

The **FePd-2**, **FePd-3** and **FePd-4** NPs were characterized by powder XRD. As depicted in Fig. 6, all of them have a chemically ordered structure, which can be deduced from the characteristic peaks (001) and (110) and the splitting of (200) and (202) peaks. In addition, broadening of the (111) peak from **FePd-2** to **FePd-4** matched with the change of the sample size, and the average crystallite sizes estimated from the peak broadening at (111) plane using the Scherrer formula were 10.9, 14.2 and 17.9 nm for **FePd-2**, **FePt-3** and **FePt-4**, respectively. The calculated particle size and their variation agreed with the TEM analysis.

The ferromagnetic properties of **FePd-2**, **FePd-3** and **FePd-4** NPs were investigated at room temperature by VSM. The hysteresis loops in Fig. 7 reveal that the resultant NPs have chemically ordered fct phase, which are consistent with the XRD results. The coercivity values of **FePd-2**, **FePd-3** and **FePd-4** NPs were 0.95, 1.87 and 1.41 kOe, and the variation may be ascribed to the size effect of FePd NPs, because the sample size can induce the change between the multivariant mode and the single variant mode [12], [42].

3. Experimental section

3.1. General procedures

All the reactions were carried out under an atmosphere of nitrogen using standard Schlenk techniques, although no special precautions were taken to exclude air or moisture during workup except for the polymerization process. Solvents used in the polymer synthesis were dried and distilled from appropriate drying agents, followed by degassing before use. Styrene and 4-vinylpyridine were distilled from calcium hydride and *α,α'-azoisobutyronitrile* (AIBN) was recrystallized three times in EtOH before use. Other reagents were purchased and used as received.

All the reactions were monitored by thin-layer chromatography (TLC) with Merck pre-coated glass plates. Compounds were visualized with UV light irradiation at 254 and 365 nm. Purification of products was achieved by silica column chromatography. NMR spectra were measured in $CDCl_3$ or d_6-DMSO on a Bruker AV 400 NMR instrument with chemical shifts being referenced against tetramethylsilane as the internal standard for ^{1}H and ^{13}C NMR data. The molecular weight of the polymer was determined by Gel Permeation Chromatography (GPC) using a HP 1050 series HPLC instrument with visible wavelength and fluorescent detectors against polystyrene standards. IR spectra were recorded on the Nicolet Magna 550 Series II FTIR spectrometer using KBr pellets for solid state spectroscopy. Thermal analyses were performed with a Perkin-Elmer TGA 6 thermal analyzer.

The structural characterization of the as-synthesized FePd NPs was performed by powder XRD on a Bruker AXS D8 Advance X-Ray Diffractometer, with Cu Kα (running condition: 40 kV, 40 mA) for analyzing the composition and phase purity of the resulting NPs, TEM on a Philips Tecnai G2 20S-TWIN Transmission Electron Microscope for probing the morphology,

particle size and size distribution of NPs, EDX on a fully embedded EDAX detector on TEM for composition analysis and VSM was applied for the magnetic hysteresis loops of FePd NPs. For the single-crystal analysis of **TPy-FePd-1**, X-ray diffraction data were collected at 173 K using graphite-monochromated Mo-*K*α radiation (λ = 0.71073 Å) with a Bruker APEX II CCD diffractometer. The collected frames were processed with the software SAINT+ [43] and an absorption correction (SADABS) [44] was applied to the collected reflections. The structure was solved by direct methods (SHELXTL) [45] in conjunction with standard difference Fourier techniques and subsequently refined by full-matrix least-squares analyses on F^2. Hydrogen atoms were generated in their idealized positions and all non-hydrogen atoms were refined anisotropically. CCDC-1530670 contains the supplementary crystallographic data for this paper. These data can be obtained free of charge from The Cambridge Crystallographic Data Center via www.ccdc.cam.ac.uk/data_request/cif.

3.2. Synthesis of 4′-(ferrocenyl)-[2,2′:6′,2″]terpyridine

The synthesis of 4′-(ferrocenyl)-[2,2′:6′,2″]terpyridine was previously reported by using the traditional two-step synthetic route. In this study, we adopted a new one-step reaction starting from the readily available ferrocenecarboxaldehyde and 2-acetylpyridine to get the target compound. 2-Acetylpyridine (0.727 g, 6 mmol) was first added into a solution of ferrocenecarboxaldehyde (0.642 g, 3 mmol) in EtOH (40 mL). KOH pellets (0.455 g, 85%, 8.1 mmol) and aq. NH_3 (11.4 mL, 28%) were then added into the solution. The solution was stirred at 50 °C for 24 h. The mixture was then cooled to 20 °C and the solid formed was collected by filtration and washed with ice-cold EtOH (10 mL). Recrystallization from EtOH afforded a dark red crystalline solid (4.2 g, 13.0 mmol, 65%). ^{1}H NMR ($CDCl_3$, 400 Hz, δ/ppm) 8.75 (d, J = 4.7 Hz, 2H, Ar), 8.68 (d, J = 7.9 Hz, 2H, Ar), 8.57 (s, 2H, Ar-H), 7.97 (td, J = 7.8,

1.8 Hz, 2H, Ar), 7.46 (dd, *J* = 6.9, 5.3 Hz, 2H, Ar), 5.12–4.90 (m, 2H, C_5H_4), 4.59–4.41 (m, 2H, C_5H_4), 4.11 (s, 5H, C_5H_5). MALDI-TOF-MS: *m*/*z* calcd for $C_{25}H_{19}FeN_3$: 417.09, found: 417.09 $[M]^+$.

3.3. Synthesis of TPy-FePd-1

To $Pd(OAc)_2$ (0.45 g, 2 mmol, 1.0 equiv) in MeCN (10 mL) at room temperature was added 4′-(ferrocenyl)-[2,2′:6′,2″]terpyridine (0.83 g, 2 mmol, 1.0 equiv). The reaction mixture was stirred for 1 h, affording a dark blue slurry. To this slurry was added $HBF_4{\cdot}OEt_2$ (0.6 mL, 4.1 mmol, 2.05 equiv) via syringe. The reaction mixture was stirred vigorously for 30 min, and then 50 mL of Et_2O was poured into the mixture to precipitate the product. The solid was collected by filtration and washed with Et_2O (100 mL). The filtrate was dissolved in a small amount of acetonitrile and precipitated in Et_2O, and the precipitation process was repeated for three times to get the pure product as a dark green solid (90% yield). X-ray quality crystals were also grown from MeCN/Et_2O. ^{1}H NMR (*d*$_6$-DMSO, 400 Hz, *δ*/ppm) 8.84 (d, *J* = 7.6 Hz, 2H, Ar), 8.61 (s, 3H, Ar), 8.56 (d, *J* = 8.0 Hz, 3H, Ar), 7.96 (t, *J* = 7.2 Hz, 2H, Ar), 5.47 (s, 2H, C_5H_4), 4.88 (s, 2H, C_5H_4), 4.20 (s, 5H, C_5H_5). MALDI-TOF-MS: *m*/*z* calcd for $[M\text{-MeCN-}2BF_4]^+$: 522.01, found: 522.14 $[M\text{-MeCN-}2BF_4]^+$. T_{onset} = 247 °C. The structure in the solid state was identified by single crystal X-ray analysis.

3.4. Synthesis of TPy-FePd-2

To a stirred mixture of **TPy-FePd-1** (0.6 g, 1 mmol) in anhydrous MeCN (20 mL), 4-*tert*-butylpyridine (0.16 mg, 1.2 mmol) was added in one portion, and the mixture was stirred vigorously for 1 h to get the title product as a purple-black solid in quantitative yield. ^{1}H NMR (*d*$_6$-DMSO, 400 Hz, *δ*/ppm) 9.07 (s, 2H, Ar), 8.89 (d, *J* = 8.0 Hz, 2H, Ar), 8.67 (s, 2H, Ar), 8.57–

8.53 (m, 2H, Ar), 7.97 (s, 2H, Ar), 7.82 (t, J = 6.4 Hz, 2H, Ar), 7.68 (s, 2H, Ar), 5.50 (s, 2H, C_5H_4), 4.90 (s, 2H, C_5H_4), 4.22 (s, 5H, C_5H_5), 1.42 (s, 9H, CH_3).

3.5. Synthesis of PS-P4VP

This block copolymer was synthesized by the free radical polymerization. In this reaction, styrene (1.8 g, 17.3 mmol), 4-vinylpyridine (1.96 g, 17.3 mmol) and AIBN (295 mg, 5 mol%) in 5 mL of THF were combined in a 25 mL Schlenk tube and degassed by subjecting the mixture to three freeze-dry-thaw cycles under nitrogen. The mixture was heated under 80 °C for 15 h and then cooled to room temperature. The resulting polymer was dissolved in a minimum volume of THF, precipitated in methanol (100 mL), and centrifuged to separate the compound. After precipitation for three times by using a THF-methanol system, the white solid collected was dried under high vacuum to obtain the target product. The ratio of blocks was found to be 1:1 PS:P4VP by ^{1}H NMR. ^{1}H NMR ($CDCl_3$, 400 MHz, δ/ppm) 8.28 (s, Ar), 7.08 (s, Ar), 6.41 (s, Ar), 1.58–1.23 (m, polymer backbone). M_n = 11830, M_w = 16550, PDI = 1.40.

3.6. Synthesis of P1, P2 and P3

In a typical run, to a stirred mixture of **TPy-FePd-1** in anhydrous MeCN (20 mL) was added the solution of **PS-P4VP** in DMF, and the mixture was stirred vigorously for 1 h to get the title product as a solid in quantitative yield. The metal fraction in polymer was controlled by tuning the amount of **TPy-FePd-1 (**5 wt%, 10 wt% and 20 wt% for **P1**, **P2** and **P3**, respectively**)**. The final products **P1**, **P2** and **P3** were characterized by ^{1}H NMR spectroscopy to determine the ratio of metal fraction in the polymer chain.

3.7. Preparation of FePd NPs

The FePd alloy NPs were prepared by direct pyrolysis of the respective precursors under an Ar/H_2 (5 wt%) atmosphere. The organometallic single-source precursors were placed in a

ceramic boat inside a quartz tube in a furnace. The tube was purged with gas under an Ar/H_2 atmosphere and heated to the desired temperature of 500 °C at a rate of 10 °C/min and held for 1 h. After cooling to room temperature, the tube was then heated to 800 °C and held for 1 h. Finally, ferromagnetic FePd NPs were formed.

4. Conclusions

To conclude, Fe,Pd-containing bimetallic polymers were successfully used as single-source precursors to prepare ferromagnetic FePd NPs by a one-pot pyrolysis method. The resultant NPs had chemically ordered fct phase and exhibited excellent magnetic properties. Also, the size of the NPs could be tuned by controlling the ratio of metal fraction in the polymer, which provided a possibility of size tuning of NPs by the proper design of the bimetallic precursors.

Acknowledgements

C.-L. Ho thanks Hong Kong Research Grants Council (HKBU12317216), Hong Kong Baptist University (FRG1/15-16/043 and FRG2/15-16/074), the Science, Technology and Innovation Committee of Shenzhen Municipality (JCYJ20160531193836532) and the National Natural Science Foundation of China (21504074) for their financial support. W.-Y. Wong acknowledges the financial support from the National Natural Science Foundation of China (51373145), Hong Kong Research Grants Council (HKBU203312), Areas of Excellence Scheme, University Grants Committee of HKSAR (AoE/P-03/08) and the Hong Kong Polytechnic University (1-ZE1C). C.-W. Leung acknowledges the support of RGC-GRF (The Hong Kong Polytechnic University 153015/14P) and The Hong Kong Polytechnic University (1-ZE25). The present work was also supported by the Inter-institutional Collaborative Research Scheme of Hong Kong Baptist University (RC-ICRS/14-15/02).

Graphical abstract

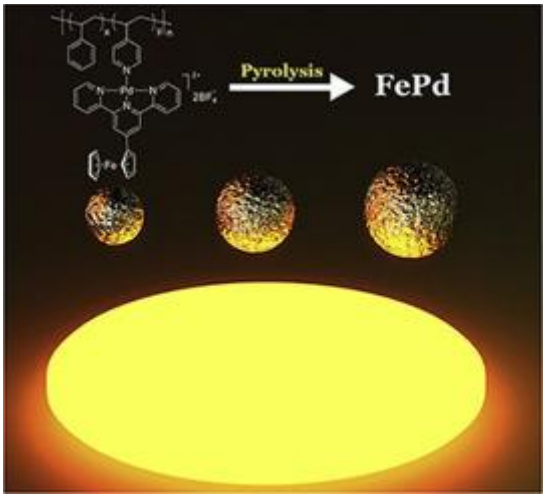

A bimetallic complex **TPy-FePd-1** was used as a single-source precursor to synthesize ferromagnetic FePd nanoparticles by a one-pot pyrolysis. In addition, metallopolymers with different metal fractions derived from **TPy-FePd-1** were prepared and the size of FePd NPs from these polymer precursors increased linearly with the metal content.

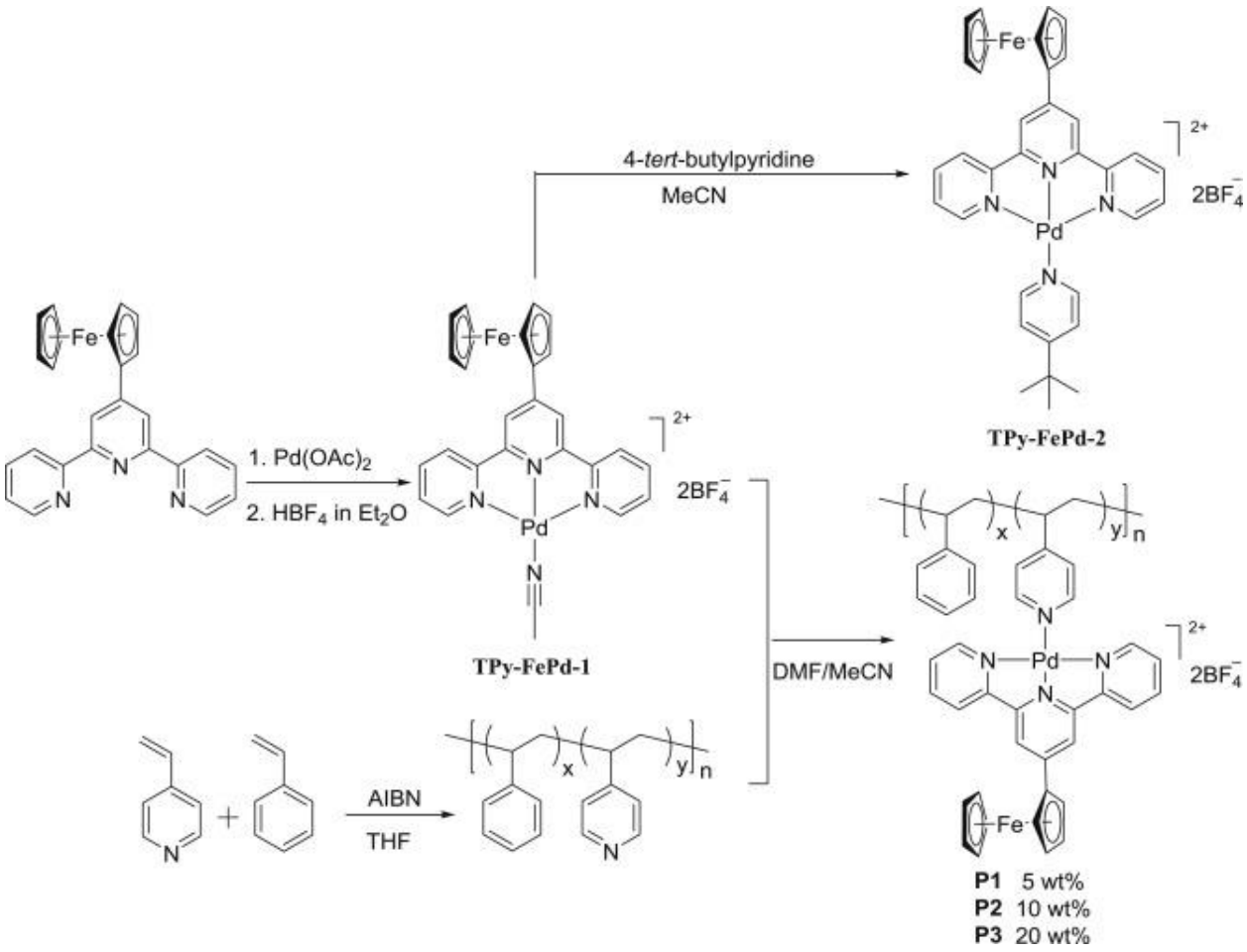

Scheme 1. Synthetic routes for bimetallic precursor **TPy-FePd-1** and copolymers **P1–P3**.

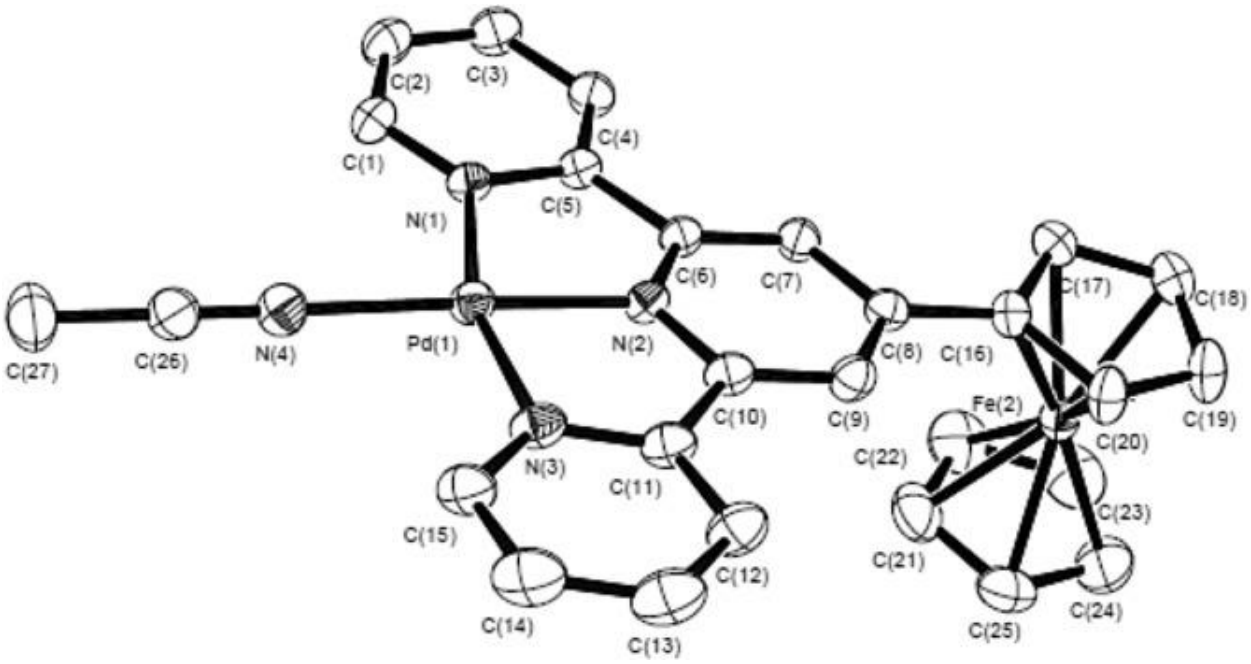

Fig. 1. Molecular structure of **TPy-FePd-1** presented by an ORTEP diagram. All hydrogen atoms are omitted for clarity.

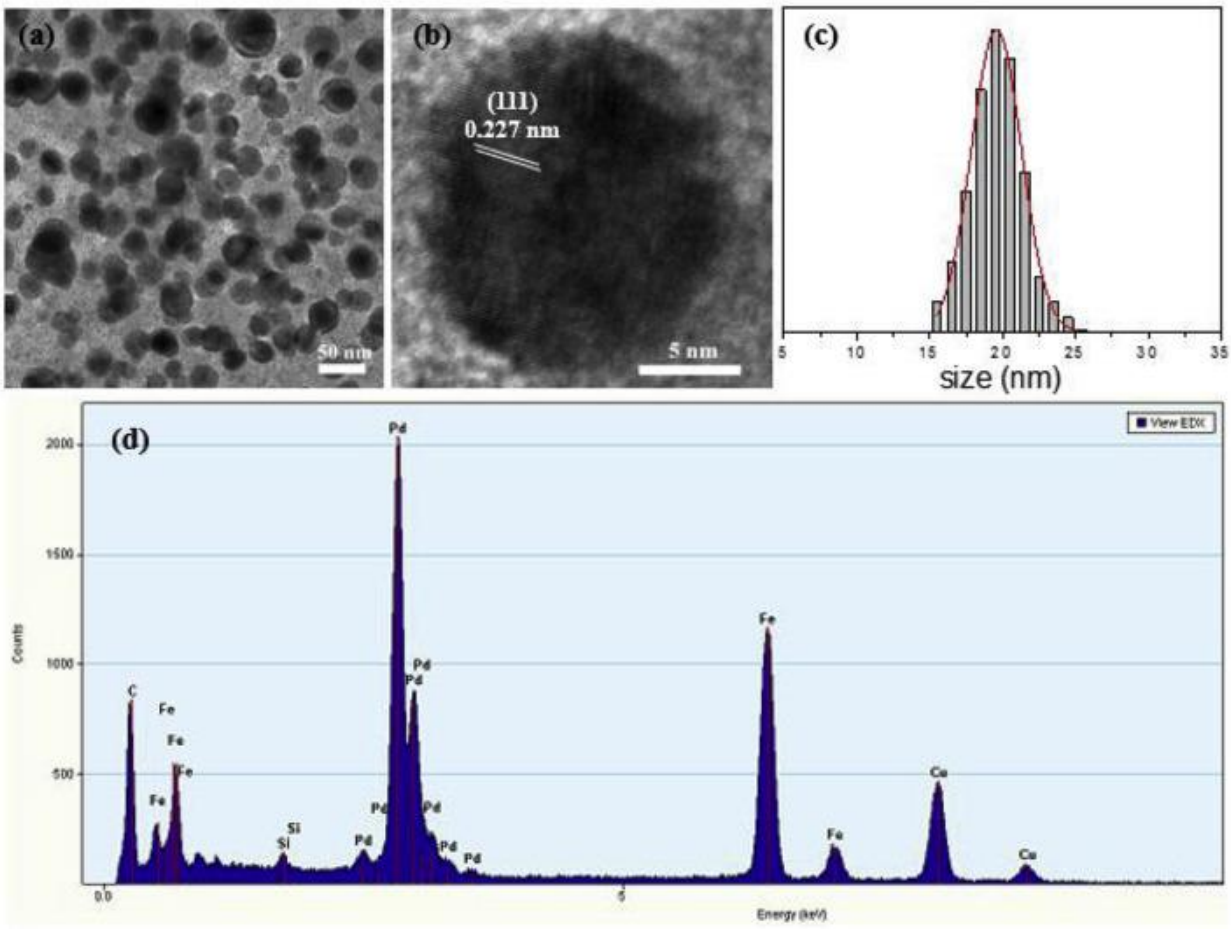

Fig. 2. (a) Low-resolution and (b) high-resolution TEM images of **FePd-1** NPs; (c) size distribution histogram statistically analyzed from the TEM image in (a); (d) EDX spectrum of **FePd-1** NPs.

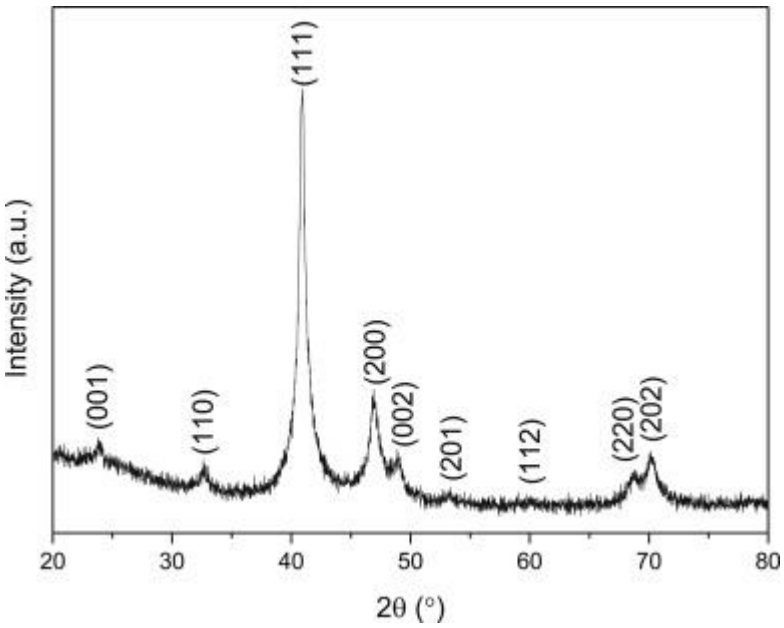

Fig. 3. Powder XRD plot of the as-synthesized **FePd-1** NPs.

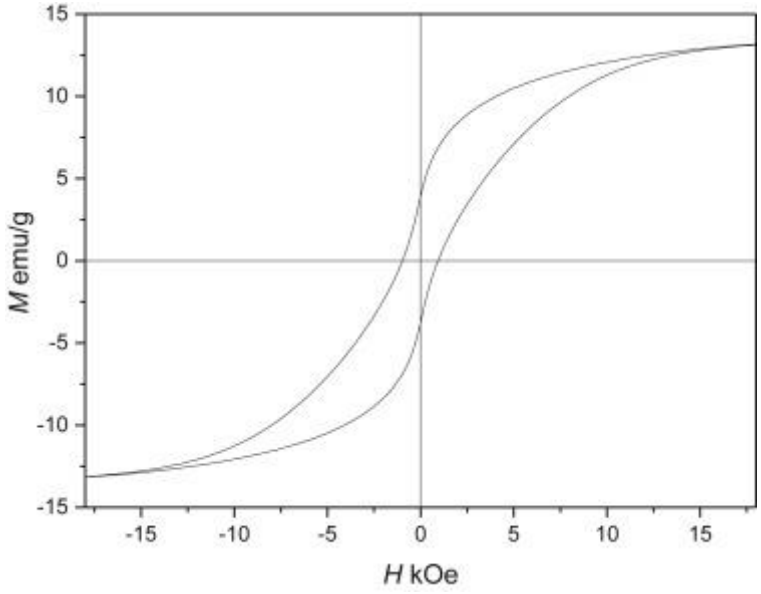

Fig. 4. Room temperature hysteresis loop of the resultant **FePd-1** NPs.

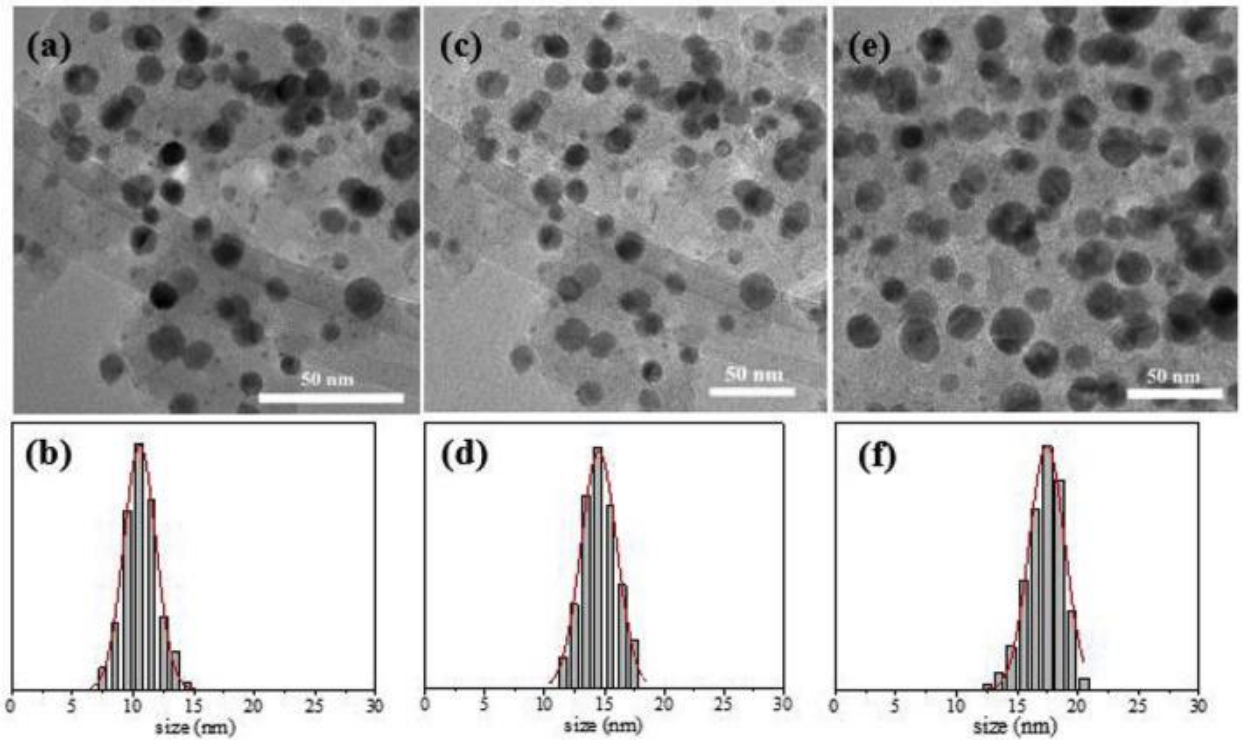

Fig. 5. TEM images and size distribution histograms of (a–b) **FePd-2**, (c–d) **FePd-3** and (e–f) **FePd-4**.

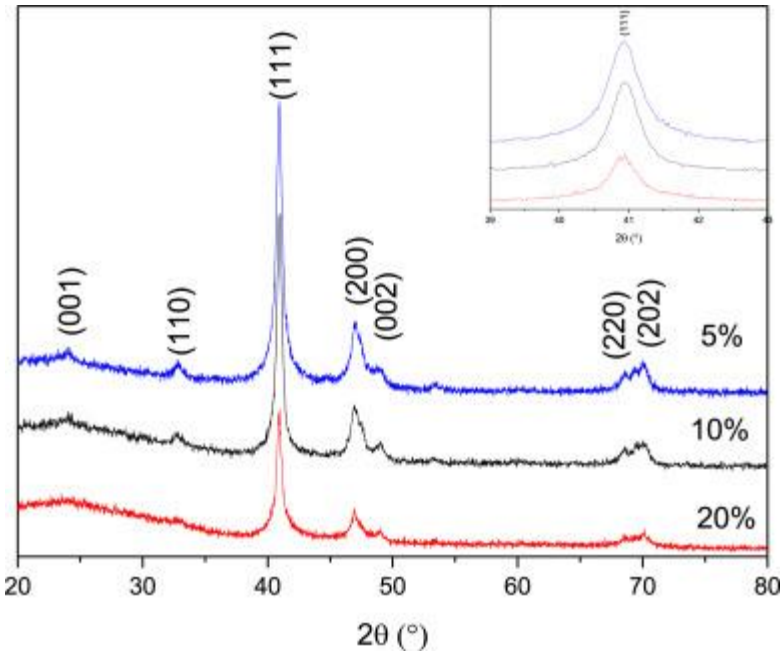

Fig. 6. Powder XRD patterns of the as-synthesized **FePd-2**, **FePd-3** and **FePd-4** NPs.

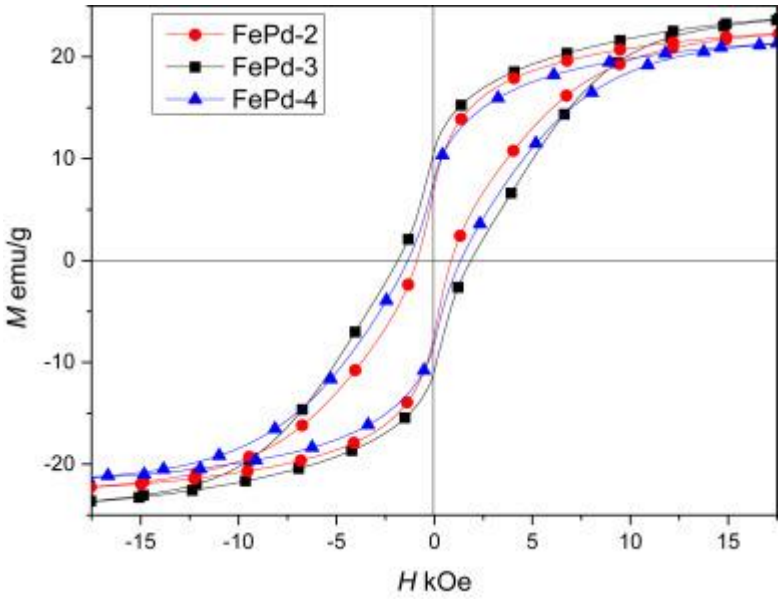

Fig. 7. Room temperature hysteresis loops of **FePd-2**, **FePd-3** and **FePd-4** NPs.

Table 1. Selected bond lengths (Å) and angles (°) for **TPy-FePd-1**.

	length		**angle**
Pd(1)-N(2)	1.922(2)	N(2)-Pd(1)-N(4)	176.43(11)
Pd(1)-N(4)	2.015(3)	N(2)-Pd(1)-N(1)	80.77(10)
Pd(1)-N(1)	2.030(2)	N(4)-Pd(1)-N(1)	98.15(10)
Pd(1)-N(3)	2.031(2)	N(2)-Pd(1)-N(3)	80.89(10)
		N(4)-Pd(1)-N(3)	100.29(11)
		N(1)-Pd(1)-N(3)	161.53(10)

References

[1] H.K. Chao, R.A. Riggleman, Polymer 54 (2013) 5222e5229.

[2] D.E. Garcia, D. Hotza, Mater. Lett. 82 (2012) 88e90.

[3] A.A. Gavrilov, A.V. Chertovich, P.G. Khalatur, A.R. Khokhlov, Soft Matter 9 (2013) 4067e4072.

[4] V. Subramanian, E.E. Wolf, P.V. Kamat, J. Am. Chem. Soc. 126 (2004) 4943e4950.

[5] S.L. Zhang, Y. Zhang, Z. Fu, S.N. Wu, M. Gao, M. Liu, J. Chen, L. Niu, J.Z. Jiang, Y. Ling, Q. Wang, H. Chen, Appl. Phys. Lett. 89 (2006) 243108.

[6] Y.P. He, Y.M. Miao, C.R. Li, S.Q. Wang, L. Cao, S.S. Xie, G.Z. Yang, B.S. Zou, C. Burda, Phys. Rev. B 71 (2005) 125411.

[7] T.S. Chan, R.S. Liu, C.C. Yang, W.H. Li, Y.H. Lien, C.Y. Huang, J.F. Lee, J. Phys. Chem. B 111 (2007) 2262e2267.

[8] A. Ceylan, C.C. Baker, S.K. Hasanain, S.I. Shah, J. Appl. Phys. 100 (2006) 034301.

[9] X.H. Chen, H.T. Zhang, C.H. Wang, X.G. Luo, P.H. Li, Appl. Phys. Lett. 81 (2002) 4419e4421.

[10] T. Appenzeller, Science 254 (1991) 1300e1301.

[11] H. Shima, K. Oikawa, A. Fujita, K. Fukamichi, K. Ishida, A. Sakuma, Phys. Rev. B 70 (2004) 224408.

[12] K. Seki, H. Kura, T. Sato, T. Taniyama, J. Appl. Phys. 103 (2008) 063910.

[13] K. Sato, B. Bian, Y. Hirotsu, J. Appl. Phys. 91 (2002) 8516e8518.

[14] H.L. Nguyen, L.E.M. Howard, S.R. Giblin, B.K. Tanner, I. Terry, A.K. Hughes, I.M. Ross, A. Serres, H. Burckstummer, J.S.O. Evans, J. Mater. Chem. 15 (2005) 5136e5143.

[15] N.S. Gajbhiye, S. Sharma, R.S. Ningthoujam, J. Appl. Phys. 104 (2008) 123906.

[16] K. Mori, Y. Kondo, H. Yamashita, Phys. Chem. Chem. Phys. 11 (2009) 8949e8954.

[17] B.Z. Cui, M. Marinescu, J.F. Liu, J. Appl. Phys. 114 (2013) 223903.

[18] F. Pan, T. Yang, J. Zhang, B.X. Liu, J. Phys. 5 (1993) L507eL514.

[19] K.S. Suslick, M.M. Fang, T. Hyeon, J. Am. Chem. Soc. 118 (1996) 11960e11961.

[20] S.H. Sun, C.B. Murray, D. Weller, L. Folks, A. Moser, Science 287 (2000) 1989e1992.

[21] Y.L. Hou, H. Kondoh, T. Kogure, T. Ohta, Chem. Mater. 16 (2004) 5149e5152.

[22] G.S. Chaubey, C. Barcena, N. Poudyal, C.B. Rong, J.M. Gao, S.H. Sun, J.P. Liu, J. Am. Chem. Soc. 129 (2007) 7214e7215.

[23] Z.T. Zhang, D.A. Blom, Z. Gai, J.R. Thompson, J. Shen, S. Dai, J. Am. Chem. Soc. 125 (2003) 7528e7529.

[24] Y.S. Yu, K.W. Sun, Y. Tian, X.Z. Li, M.J. Kramer, D.J. Sellmyer, J.E. Shield, S.H. Sun, Nano Lett. 13 (2013) 4975e4979.

[25] O. Metin, A. Mendoza-Garcia, D. Dalm € ızrak, M.S. Gültekina, S.H. Sun, Catal. Sci. Technol. 6 (2016) 6137e6143.

[26] M. An, X.G. Yan, Z.Z. Tian, J. Zhao, B.A. Liu, F.F. Dang, X.L. Yang, Y. Wu, G.J. Zhou, Y.X. Ren, L.J. Gao, J. Mater. Chem. C 4 (2016) 5626e5633.

[27] B.A. Liu, Z.Z. Tian, F.F. Dang, J. Zhao, X.G. Yan, X.B. Xu, X.L. Yang, G.J. Zhou, Y. Wu, J. Organomet. Chem. 804 (2016) 80e86.

[28] Z. Huang, B.A. Liu, J. Zhao, Y. He, X.G. Yan, X.B. Xu, G.J. Zhou, X.L. Yang, Z.X. Wu, RSC Adv. 5 (2015) 36507e36519.

[29] Z. Huang, B.A. Liu, J. Zhao, Y. He, X.G. Yan, X.B. Xu, G.J. Zhou, X.L. Yang, Z.X. Wu, RSC Adv. 5 (2015) 12100e12110.

[30] Z.Q. Zhu, S.W. Wang, J. Du, Q. Jin, T.R. Zhang, F.Y. Cheng, J. Chen, Nano Lett. 14 (2014) 153e157.

[31] A. Capobianchi, M. Colapietro, D. Fiorani, S. Foglia, P. Imperatori, S. Laureti, E. Palange, Chem. Mater. 21 (2009) 2007e2009.

[32] M.S. Wellons, W.H. Morris, Z. Gai, J. Shen, J. Bentley, J.E. Wittig, C.M. Lukehart, Chem. Mater. 19 (2007) 2483e2488.

[33] H.M. Song, J.H. Hong, Y.B. Lee, W.S. Kim, Y. Kim, S.J. Kim, N.H. Hur, Chem. Commun. 12 (2006) 1292e1294.

[34] A.D. Russell, G.R. Whittell, M.F. Haddow, I. Manners, Organometallics 33 (2014) 5349e5357.

[35] Q. Dong, G. Li, C.-L. Ho, M. Faisal, C.-W. Leung, P.-W. Pong, K. Liu, B.Z. Tang, I. Manners, W.-Y. Wong, Adv. Mater. 24 (2012) 1034e1040.

[36] K. Liu, C.-L. Ho, S. Aouba, Y.Q. Zhao, Z.H. Lu, S. Petrov, N. Coombs, P. Dube, H.E. Ruda, W.-Y. Wong, I. Manners, Angew. Chem. Int. Ed. 47 (2008) 1255e1259.

[37] Z.-G. Meng, G.J. Li, S.M. Ng, H.F. Wong, S.-C. Yiu, C.-L. Ho, C.-W. Leung, W.- Y. Wong, Polym. Chem. 7 (2016) 4467e4475.

[38] Z.-G. Meng, G.J. Li, H.F. Wong, S.M. Ng, S.-C. Yiu, C.-L. Ho, C.W. Leung, I. Manners, W.-Y. Wong, Nanoscale 9 (2017) 731e738.

[39] Q. Dong, G.J. Li, H. Wang, P.-W. Pong, C.-W. Leung, I. Manners, C.-L. Ho, H. Li, W.-Y. Wong, J. Mater. Chem. C 3 (2015) 734e741.

[40] Q. Dong, W.S. Qu, W.Q. Liang, F.F. Tai, K.P. Guo, C.-W. Leung, Y.-H. Lo, W.- Y. Wong, J. Mater. Chem. C 4 (2016) 5010e5018.

[41] E. Kang, H. Jung, J.G. Park, S. Kwon, J. Shim, H. Sai, U. Wiesner, J.K. Kim, J. Lee, ACS Nano 5 (2011) 1018e1025.

[42] B. Issa, I.M. Obaidat, B.A. Albiss, Y. Haik, Int. J. Mol. Sci. 14 (2013) 21266e21305.

[43] SAINTþ, Ver. 6.02a, Bruker Analytical X-ray System, Inc., Madison, WI, 1998.

[44] G.M. Sheldrick, SADABS, Empirical Absorption Correction Program, University of Gottingen, Germany, 1997 € .

[45] G.M. Sheldrick, SHELXTLTM, Reference Manual, Ver. 5.1, 1997. Madison, WI.